UNIVERSITY OF TWENTE.

Faculty of Science and Technology,
Technical Medicine,
Medical Sensing & Stimulation

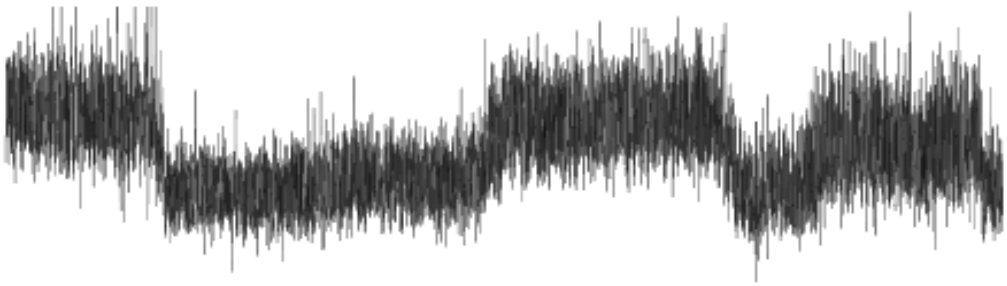

Amplitude integrated electroencephalography analysis of sleep architecture in mechanically ventilated children

Douwe van der Steen

M.Sc. Thesis
December 2021

Supervisors:
prof. dr. D.W. Donker
dr. M.C.J. Kneyber
dr. E. Mos - Oppersma
drs. P.A. van Katwijk
drs. R.G.T. Blokpoel
drs. A.A. Koopman

Beatrix Kinderziekenhuis
Universitair Medisch Centrum Groningen

Amplitude integrated electroencephalography analysis of sleep architecture in mechanically ventilated children

Master Thesis

Douwe van der Steen
Technical medicine
Medical Sensing and Stimulation
09 December 2021

Graduation committee

Chairman:
prof.dr. D.W. Donker

Technical supervisor UT:
dr. E.Mos - Oppersma

Medical supervisors:
dr. M.C.J. Kneyber
drs. R.G.T. Blokpoel

Process supervisor:
drs. P.A. van Katwijk

External member UT:
dr. A.T.M. Bellos – Grob

Summary

Objective First, characterise aEEG background patterns and sleep-wake cycling during mechanical ventilation in a heterogeneous group of critically ill children. Second, to create a simple detection algorithm for the presence of sleep-wake cycles in a three hour period.
Design Secondary analysis of physiology data.
Setting Tertiary paediatric intensive care unit in a university hospital.
Patients Mechanically ventilated children $<$ 18 years of age in whom the bedside team indicated aEEG monitoring, i.e., established or suspected epileptic activity, depressed level of consciousness, hypoxic-ischemic encephalopathy, (postoperative) congenital heart disease, extracorporeal membrane oxygenation, significant neurological malformations, meningitis, and use of continuous neuromuscular blockade.
Measurements and Main Results Three-hour sections of aEEG during the night were used for analysis. A total of 115 patients were included, this resulted in 617 aEEG sections. The sections were classified into different background patterns and on the presence of sleep-wake cycling. The results showed a mix of CNV and DNV in the 0-1 month group, but predominantly CNV in the older age groups. The amplitude of the CNV upper and lower bands showed an increasing trend with increasing age. An increase in ventilation days was correlated with lower aEEG amplitudes. SWC were seen in all age groups, however, after two years of age, a sudden drop in SWC occurrence was observed. The detection algorithm, which used two outcome variables (no SWC or some form of SWC), had an accuracy of 87.7%.
Conclusion The amplitude of the aEEG bands increases with age, and SWC are commonly seen until two years. The automated detection of SWC is promising and could be helpful in further research.

Contents

List of acronyms

PICU	paediatric intensive care unit
NICU	neonatal intensive care unit
PSG	Polysomnography
aEEG	amplitude integrated electroencephalography
CFM	cerebral function monitor
CNV	continuous normal voltage
DNV	discontinuous normal voltage
BS	burst suppression
LV	low voltage
FT	flat tract
SWC	sleep-wake cycles
REM	rapid eye movement
NREM	non-rapid eye movement
EEG	electroencephalography
EMG	electromyography
EOG	electro-oculography
AS	active sleep
QS	quiet sleep
IS	indeterminate sleep
LVI	low voltage irregular
M	mixed activity
HVS	high voltage slow wave
TA	tracé alternate
PIM	Pediatric Index of Mortality
PRISM	Pediatric RISk of Mortality
ApEN	approximate entropy

SVM support vector machine

AUC area under the curve

SD standard deviation

IQR interquartile range

Chapter 1

Introduction

Paediatric critical care medicine is a subspecialty for children with life-threatening conditions. Unfortunately, admission to the paediatric intensive care unit (PICU) can be a stressful and turbulent situation for children who are actively going through neurocognitive development, and this inevitably leads to impaired sleep [1], [2]. While sleep is thought to play a crucial part in recovery, little research is conducted on the subject [2].

Factors influencing sleep in intensive care can be endogenously caused by the underlying disease process or exogenous like light, noise, intrusive monitoring, interventions and medication [3]. Poor sleep quality has consistently been reported in the adult and paediatric critical care literature [4]–[7]. Although the mechanisms are unknown, sleep disturbances can severely disturb the cardiovascular, respiratory, endocrine, immune, and neurologic subsystems [7]. Albeit scantily, the results of sleep investigation in the paediatric critical care show a lack of ultradian rhythm, a reduction of sleep time at night, an increase of nighttime awakenings, and a reduction of active sleep [2], [7], [8]. On top of the altered sleep in the PICU, patients can have a disturbed sleep pattern up to six months after discharge [7]. In the latest years, the importance of sleep quality in the PICU has gained increasing attention, however, the knowledge of the sleep pattern of mechanically ventilated children is still scarce [7].

The gold standard for evaluating sleep is Polysomnography (PSG). However, this is not an appropriate tool for prolonged monitoring in the PICU. It is expensive, cumbersome and the scoring is time-intensive. A recurrent alternative to PSG is Actigraphy, which utilises a wearable accelerometer to assign sleep or awake states. This method, however, has limited accuracy in mechanically ventilated children due to the higher use of sedation or neuromuscular blockade [3], [9]. A method is needed to study the sleep pattern during mechanical ventilation efficiently. amplitude integrated electroencephalography (aEEG), a method that is commonly used in the neonatal critical care, could help quantify sleep-wake cycles (SWC) and could therefore be used to study the effects of mechanical ventilation on the sleep pattern in mechanically ventilated paediatric patients [10]–[13].

1.1 Amplitude integrated EEG

aEEG is a simplified electroencephalography (EEG) measurement that can be used for prolonged monitoring of the neurological state of a patient with limited EEG electrodes. In neonatal care, it is mainly used to detect seizures, predict outcome after therapy, detect sleep-wake cycling, and detect and monitor encephalopathies [14].
The aEEG technique utilises one or two bipolar EEG montages from the 10-20 system. The EEG signal is pre-processed and filtered, a schematic explanation of the aEEG algorithm is shown in Figure 1. The obtained signals are filtered with an asymmetric bandpass filter with a cut-off frequency of 2-15Hz, this filter is designed to counteract the attenuation of the signal through the skull and scalp [15]. Then the signal is rectified and filtered again with a low-pass filter to create an envelope, which is the final aEEG signal. The signal is often time-compressed, allowing the detection of changes over a long period. The signal is displayed on a linear scale from 0-10μV and then on a logarithmic scale from 10-100μV. Due to the time compression of the signal, a band appears in the aEEG. The maximum and minimum values of this band are often used in classification, and these are called the upper and lower band of the signal. A broader bandwidth on aEEG represents repetitive changes in EEG amplitude between high and low voltage [14], [16], [17]. The signal can be classified into different classifications, but the classification introduced by Hellström-Westas et al. [18] is the most commonly used. In this classification, the aEEG is classified on three different aspects. The first aspect is the type of background activity based on amplitude and bandwidth ranging from standard to abnormal. There are five background patterns, continuous normal voltage (CNV) is the normal trace, discontinuous normal voltage (DNV) is a slightly abnormal trace, while burst suppression (BS), low voltage (LV), and flat tract (FT) are abnormal tracings [14].
The second aspect is the presence of SWC. These cycles is only seen in CNV and are sinusoidal variations of the bandwidth, mostly seen as a change in the lower band of the signal. The cycling occurs between sleep or wake state; the broader band represents activity during quiet sleep while the more narrow band represents activity during active sleep or wakefulness. There are three variations of SWC possible, no SWC, imminent/immature SWC, or developed SWC. The duration of these cycles are usually longer than 20 minutes. It is, however, unknown if these SWC are also present in the paediatric population [12], [19], [20]. The final aspect is the presence of epileptic seizure activity in the aEEG trace. An overview of these different background types and epileptic activity and the defining criteria can be seen in Figure 2.

1.2 Sleep-wake cycling

Adult sleep can be classified into different stages, and the primary division is between rapid eye movement (REM) and non-rapid eye movement (NREM). The NREM can be further subdivided into three different stages, N1, N2, and N3. Sleep can be classified in these different stages using physiological measurements, mainly EEG, electromyography (EMG),

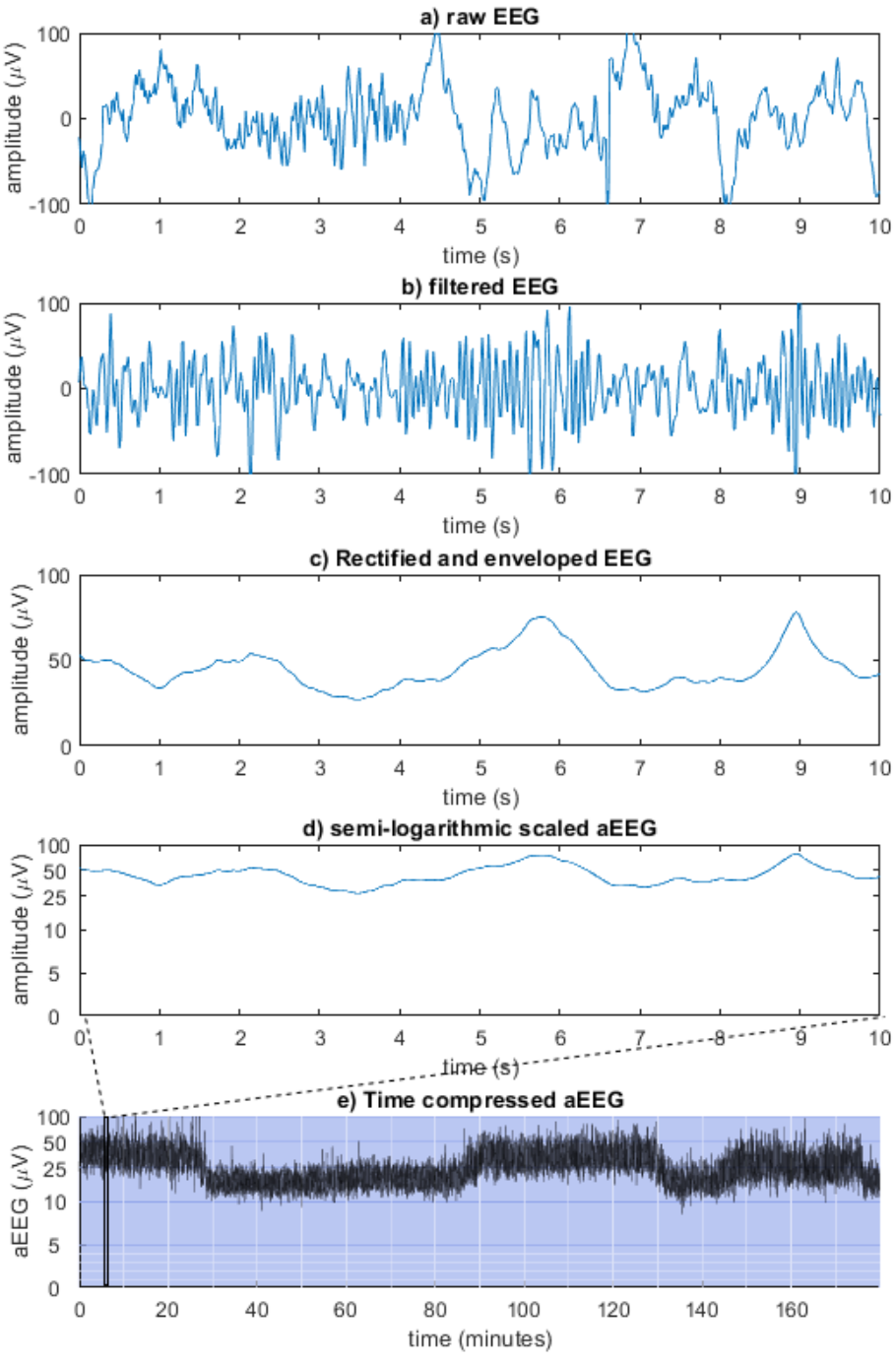

Figure 1: Visual representation of the processing steps of the aEEG algorithm.

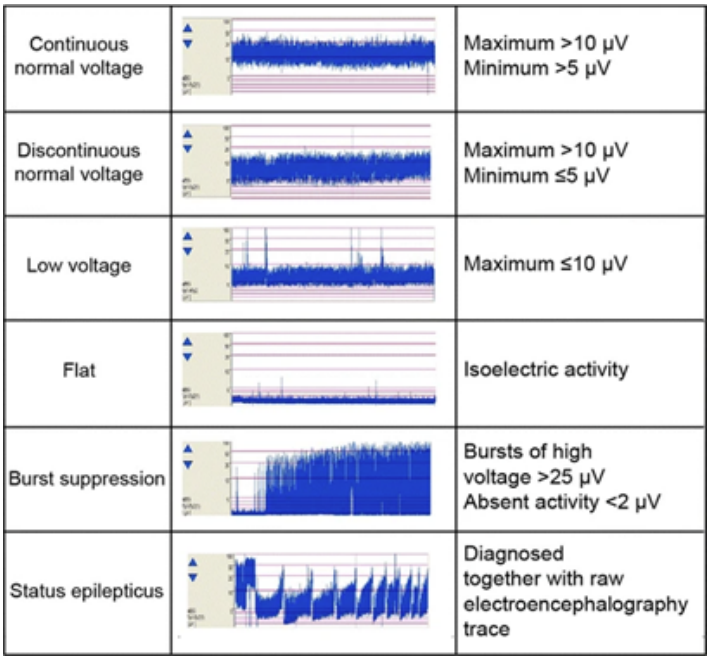

Figure 2: An overview of different types of aEEG background types, together with the defining criteria.

and electro-oculography (EOG). However, the sleep pattern in neonates differs from that of adults due to the rapidly developing brain [21]. The sleep pattern in neonates can be characterised in three different groups, active sleep (AS), quiet sleep (QS), and indeterminate sleep (IS). These groups can be classified based on different physiological measures. During active sleep, the EEG displays low voltage irregular (LVI) or mixed activity (M) patterns, and there are rapid eye movements and an irregular heart rate. AS is most similar to REM sleep in adults. Quiet sleep is mainly characterised by high voltage slow wave (HVS) and tracé alternate (TA) EEG patterns, few body movements, and regular respiratory and heart rate. QS is most reminiscent of stage N3 or slow-wave sleep in adults. Indeterminate sleep consists of characteristics of both AS and QS. A regular sleep cycle of neonates can be seen in Figure 3. This pattern is not always consistent in practice because external stimuli can easily alter sleep. The length of the sleep stages increases with age. In preterm infants, the average cycle is around 46 minutes while this increases to 115 minutes in children between 8-12 years. The neonatal sleep stages transform during the first year to the more adult sleep stages. It is recommended to apply the newborn criteria till the age of 2-6 months, and after that to change to modified adult criteria, however, this timing is not fully known [12], [19], [20].

In the aEEG signal, these changes in sleep state can be observed. During CNV, sleep-wake cycling can be seen as periodic changes in the aEEG band, mainly seen in the lower band. An example of sleep-wake cycling can be seen in Figure 4. In neonates, each cycle is at least 20 minutes in length [18]. Sleep-wake cycling in newborns is reported up to the age of three months [22]. The presence of sleep-wake cycling in older children has

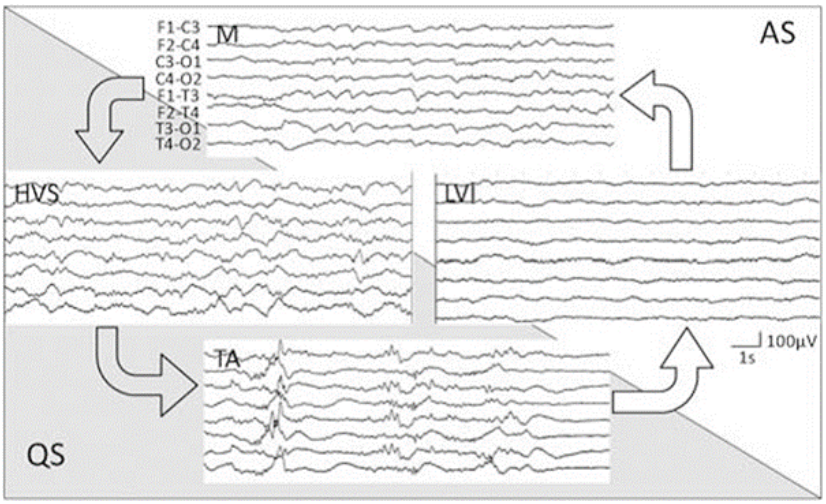

Figure 3: Different types of EEG patterns seen during a regular sleep cycle in newborns.

not been studied extensively. The name 'sleep-wake cycling' used for sinusoidal changes seen during CNV is not an appropriate name for the changes, as it does not represent the physiological states of sleep and wake. The broadening of the aEEG bandwidth represents fluctuations in the amplitude of the EEG between low and high amplitudes, which mainly represent the quiet sleep of neonates. The narrower band can represent active sleep or wake. Indeterminate sleep can occur in both the narrow and wide bands. Thus, the presence of this cyclic activity can be seen as changes in sleep states rather than the particular states of sleep and wake [13], [14], [23].

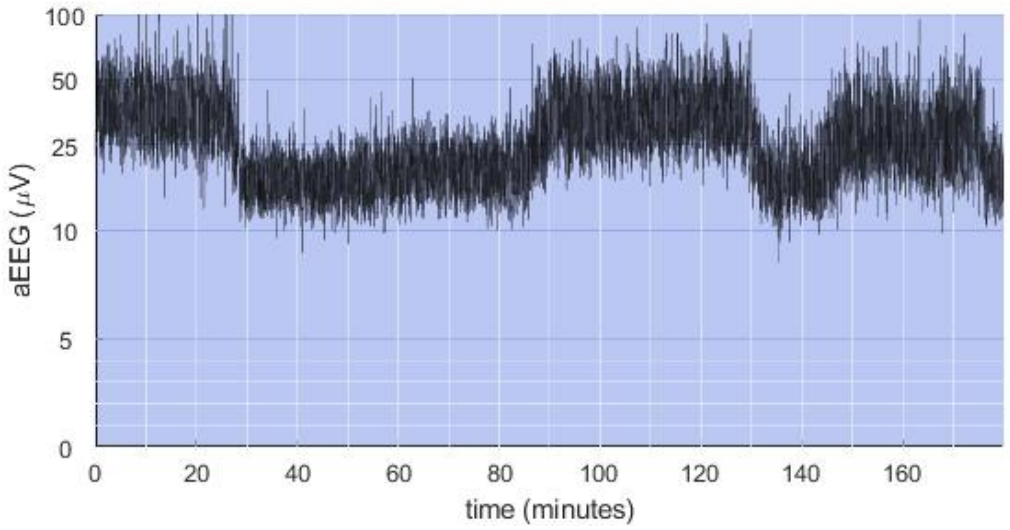

Figure 4: An example of a CNV aEEG section with SWC. The periodic changes in the aEEG band display the SWC.

1.3 aEEG in the paediatric critical care and research question

Due to its popularity in neonatal care, the technique has gained interest in the PICU. A recent questionnaire aimed at German and Swiss PICU's performed by Bruns et al. [24] showed that two-thirds of the respondents used aEEG in their paediatric population. This study showed that the primary use for the cerebral function monitor (CFM) was detecting seizures and monitoring antiepileptic treatment [25]. This is less extensive than the uses of the neonatal intensive care unit (NICU), like detecting sleep-wake cycles. This is mainly because there are no reference values available for the paediatric population. Indicating the need for better characterisation of aEEG recordings in this population [24]. This thesis will focus on two aspects of aEEG in the paediatric population.

The first aim is to characterise aEEG background patterns and sleep-wake cycling during mechanical ventilation in critically ill children and explore a relationship between the cumulative amount of sedative drugs and the duration of mechanical ventilation. This is done through a secondary analysis of prospectively collected data.

The second aim is to create a simple automatic detection algorithm for the presence of sleep-wake cycles in a three hour period.

Chapter 2

Methods

This study was designed as a secondary analysis of prospectively collected physiological data from mechanically ventilated children $<$ 18 years of age admitted to the PICU of the Beatrix Children's Hospital, University Medical Centre Groningen, in whom the clinical bedside team indicated aEEG monitoring using the Natus Olympic Brainz Monitor (Natus Medical, San Carlos, CA). There was no clinical algorithm dictating the use of aEEG, but it is custom in our unit to record aEEG when there is established or suspected epileptic activity, depressed level of consciousness, hypoxic-ischemic encephalopathy, (postoperative) congenital heart disease, extracorporeal membrane oxygenation, significant neurological malformations, meningitis, and use of continuous neuromuscular blockade for various indications. From this registry, from 2020 and then backwards included consecutive patients who had aEEG recordings for at least 3 hours during nighttime (11pm – 5am the next day). For these patients, we collected from the electronic health record (EPIC, Verona, Wisconsin) baseline demographics, including age, gender, Pediatric Index of Mortality (PIM) II and Pediatric RISk of Mortality (PRISM) II-24 hr score, and admissions diagnosis. Clinical data collected included the duration of mechanical ventilation (in days) and length of PICU stay (in days). We characterised daily use of sedatives and analgesics by expressing them as equipotential opioid or benzodiazepine dosages, respectively methadone and lorazepam, as we did previously [26], [27].

2.1 aEEG data acquisition and analysis

Both the EEG and aEEG were measured at a frequency of 200Hz and the electrical impedance of the electrodes at 100Hz. However, the Natus Olympic Brainz Monitor does not allow downloading the aEEG but only the EEG waveform to an external computer. We had to transform these EEG recordings into aEEG using the WU-NEAT model. This is an open-source Matlab (R2020b, The MathWorks Inc., Natick Massachusetts) algorithm that mimics the algorithm used in the Olympic Brainz Monitor [17]. The frequency response of the used filter can be seen in Figure 5. As the algorithm is validated for 64Hz waveforms, the EEG data were resampled from 200Hz to 64Hz.
We excluded data if the impedance was $>$ 10 kΩ and annotated interventions by the nursing

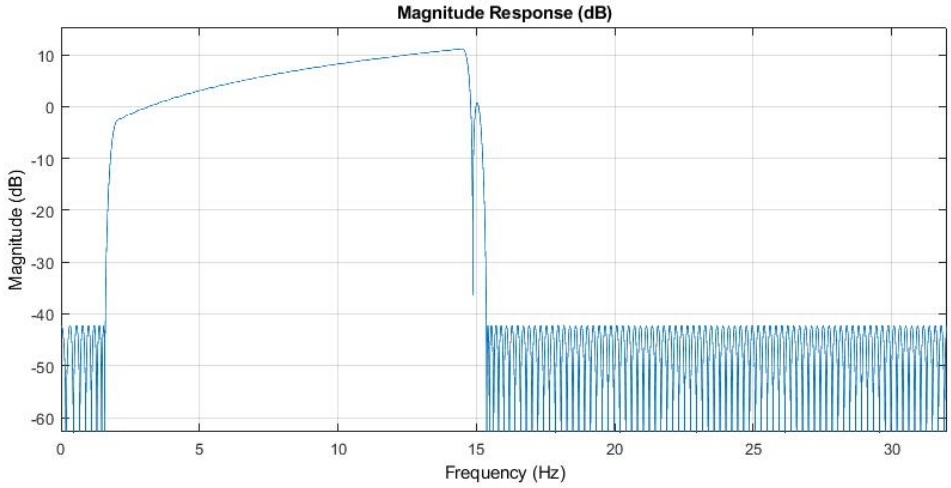

Figure 5: Frequency response of the used filter.

staff were visible. After removing this data, the files were split into two sections, each comprising three hours (11:00 pm – 02:00 am, and 02:00 am – 05:00 am). These periods were chosen to minimise artefacts in the signal due to movement or manipulation of the nursing staff. A section was not included for analysis if $>$ 30 minutes of its data was removed. We used a maximum of 10 data sections for each patient. This was to ensure that a variety of data was being used instead of the data being dominated by a few long recordings.

Then, we stratified the aEEG recordings by different background patterns using the Hellström-Westas classification: CNV, DNV, BS, LV, and FT [18]. The remaining data was labelled as indeterminate/unusable, characterised by either being sections with an abundance of previously removed data, presence of artefacts, presence of different background patterns or epileptical activity in the same data section. We considered CNV as the regular pattern, DNV as mildly abnormal, and BS, LV, and FT as severely abnormal background patterns. The presence of sleep-wake cycles was assessed in the CNV sections, allowing the sections to be labelled as ”SWC present”, ”Imminent/immature SWC”, and ”no SWC present” following the sleep-wake cycling classification of Hellström Westas [18]. A schematic overview of the pre-processing and labelling can be seen in Figure 6. Labelling was performed by one reviewer (DvdS). Thirty randomly selected sections were independently evaluated by a second reviewer (RGTB). This yielded an inter-rater agreement of 0.84 for the background patterns and 0.75 for the SWC, which is considered moderate to strong agreement [28].

The upper and lower band of the aEEG were defined for every 10 seconds by the 95th percentile (upper) and 5th percentile for the lower band (a representative example is shown in Figure 7). A moving average of 10 data points was calculated to generate the final bands. We calculated the average of the waveform, bandwidth, and the upper/lower band for each background pattern.

For the detection of SWC, all the CNV sections were used. Further calculations of the lower band were performed to serve as features of the classification model. The first calculation was to detect abrupt changes in the lower band, to mimic the classification of SWC, where

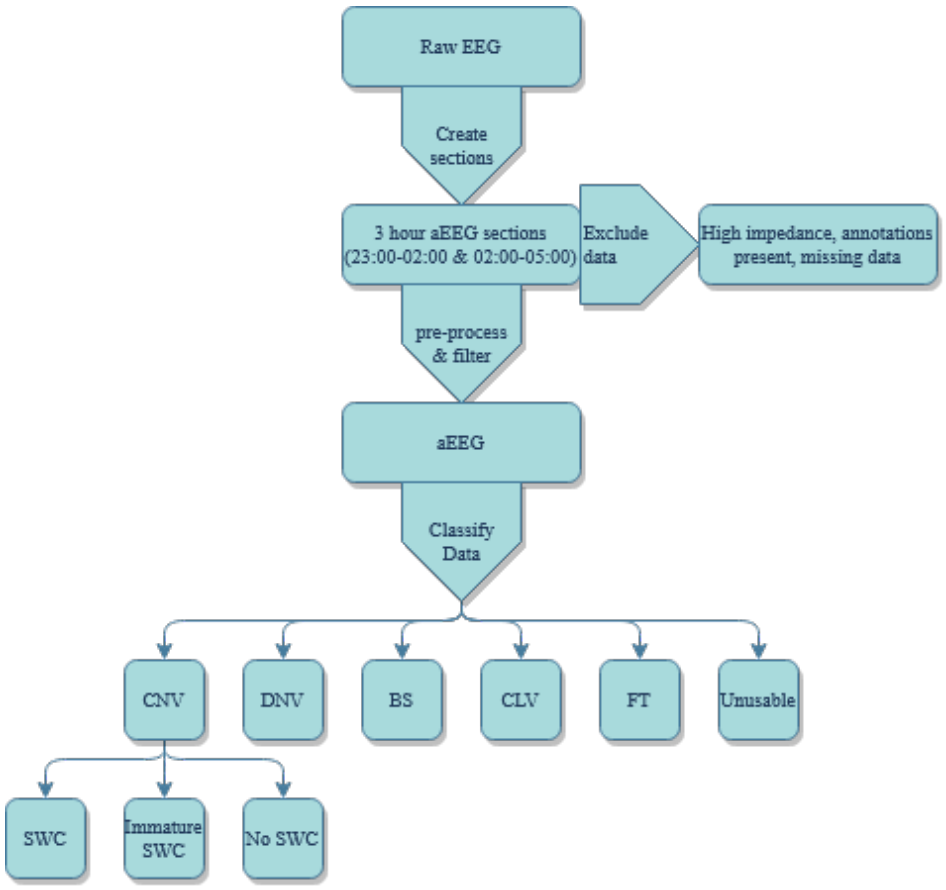

Figure 6: Schematic overview of the pre-processing and labelling steps.

SWC are characterised by sinusoidal variations, mainly in the lower band. This is done by calculating the average amplitude of five minutes of the lower band and checking if the amplitude is more than 25% different than the amplitude of the previous five minutes. This calculation is performed every 30 seconds. An example of this detection can be seen in Figure 7. The total number of abrupt changes and the number of complete cycles are calculated. One complete cycle is defined as a detected decrease in lower amplitude followed by a detected increase in lower amplitude. Furthermore, the standard deviation and the approximate entropy (ApEN) of the lower band were calculated as measures of the variability and regularity of the signal. Two classification models will be created. The first model will contain three outcome variables, 'SWC present', 'Imminent/immature SWC', and 'no SWC present'. In the second model, the 'SWC present' and 'Imminent/immature SWC' will be grouped into a new variable 'some form of SWC present'. The classification models were created with the classification learner of Matlab. Both models used a linear support vector machine (SVM) as the supervised learning model. Five-fold cross-validation was used to validate the models. The performance of the models will be scored with the accuracy, confusion matrix, and the area under the curve (AUC) of the ROC curve.

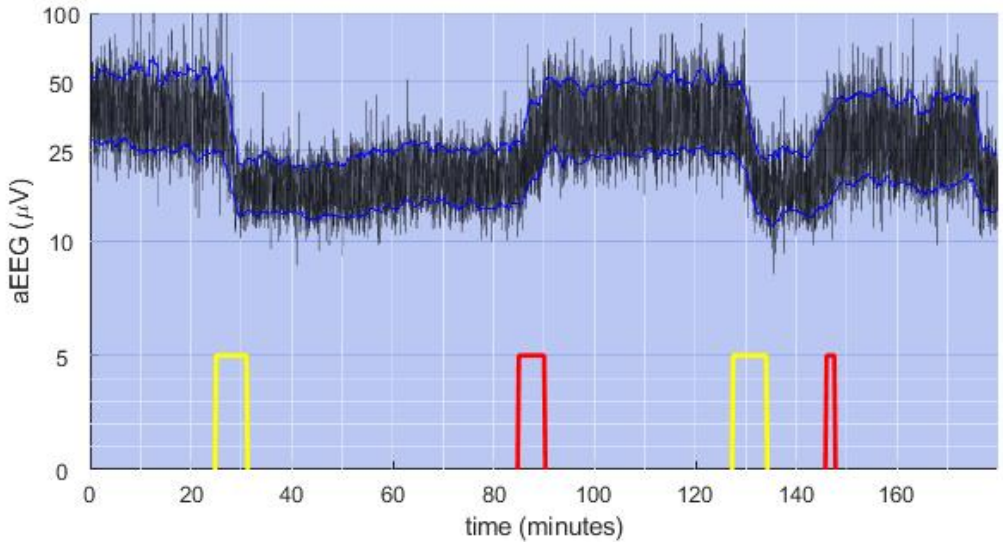

Figure 7: An example of a CNV aEEG waveform with SWC present, depicted in the black curve. The upper and lower bands are shown in the blue curve. The detected abrupt changes in the lower bands are displayed in the yellow and red curves, where a value of 5 indicates that an abrupt change has occurred. A decrease in the band is displayed in yellow, while an increase is displayed in red.

2.2 Statistical analysis

Visual inspection of QQ-plots and histograms and the Anderson-Darling test were used to test the data for normal distribution. Depending on the outcome of this test, we compared differences in continuous variables between groups using one-way ANOVA or the Kruskal-Wallis test. The chi-squared test was used for nominal or categorical variables. Descriptive data were expressed as mean $\pm$ standard deviation (SD) or median and $25-75$ interquartile range (IQR). All analyses were performed using SPSS (IBM, Chicago, Ill, USA). P values $<$ 0.05 were accepted as statistically significant.

Chapter 3

Results

One-hundred and twenty-three patients (40% of total aEEG recordings available) were included, yielding 726 sections. Eight patients and 135 sections were excluded, leaving 617 sections from 115 patients available for analysis. Table 1 summarises patient and clinical characteristics stratified by the different age groups. In the whole cohort, the median age was 4.8 months (1.2; 19.9), and 48% females. Twenty percent of the patients were admitted for acute respiratory failure, whereas 30% was admitted after cardiac surgery for congenital heart disease. The age groups up to 1 year constitute the majority of the patients. The reason for hospitalisation differed between groups, the cardiac and surgical diagnoses were mainly seen in the younger age groups. The mortality, risk scores, ventilation days, and admission days were comparable between the age groups. The dosage used for sedation was significantly different for the different age groups. CNV was observed in most sections (88%) and was not different across age strata (Figure 8). We did observe more DNV among patients 0 – 1 month old compared with other age groups. The total amount of background patterns for each age group can be found in Appendix Table 4.

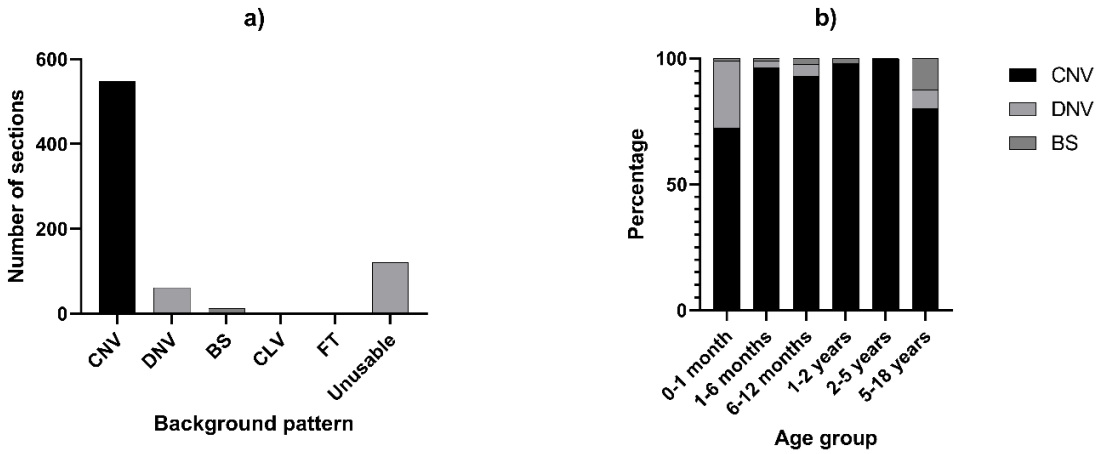

Figure 8: *a) Occurrence of each background pattern for all the sections. b) Relative occurrence of CNV, DNV & BS for each age group.*

Table 1: *Patient characteristics*

	All patients	0-1 month	1-6 months	6-12 months	1-2 years	2-5 years	5-18 years	*p*
Number of patients	115 (100)	28 (24)	37 (32)	19 (17)	12 (10)	9 (8)	10 (9)	
Number of sections	617 (100)	191 (31)	199 (32)	85 (14)	52 (8)	49 (8)	41 (7)	
Male	60 (52)	18 (64)	20 (54)	9 (53)	5 (50)	5 (56)	3 (33)	0.49
Surgical diagnosis	34 (30)	12 (43)	14 (38)	4 (21)	1 (8)	3 (33)	0 (0)	0.049
Cardiac diagnosis	26 (23)	11 (39)	9 (24)	1 (5)	2 (17)	2 (22)	1 (10)	0.11
Pulmonary diagnosis	23 (20)	3 (11)	8 (22)	6 (32)	4 (33)	1 (11)	1 (10)	0.35
Neurologic diagnosis	15 (13)	1 (4)	4 (11)	5 (26)	1 (8)	1 (11)	3 (30)	0.15
Other diagnosis	17 (15)	1 (4)	2 (5)	3 (16)	4 (33)	2 (22)	5 (50)	0.002
PIM II	-3.1 (-3.7; -1.9)	-3.1 (-3.7; -1.9)	-3.2 (-3.9; -1.9)	-3.0 (-3.7; -2.4)	-3.0 (-4.0; -2.5)	-2.5 (-3.4; -1.9)	-2.6 (-3.2; -1.3)	0.79
PRISM II	13 (8; 18)	14.5 (10.8; 17)	13 (9; 18)	10 (8; 13)	15 (10.8; 19)	12 (8; 19)	7.5 (5.5; 18.8)	0.47
Days in PICU	11 (5; 28)	13 (6; 34)	12 (4; 28)	12 (10; 37.5)	10.5 (5.5; 18.8)	7 (4; 18)	5 (2.5; 9.8)	0.22
Days on ventilator	10 (5; 21.5)	11.5 (5; 33)	7 (4; 28)	11 (7.5; 25)	9 (5.5; 12.8)	7 (5; 13)	6 (2.8; 9.3)	0.48
Mortality	22 (19)	4 (14.3)	9 (24.3)	4 (21.1)	1 (8.3)	0 (0.0)	4 (40.0)	0.22
Equipotent dosage methadone (mg/kg/day)	0.18 (0.12; 0.29)	0.12 (0.12; 0.25)	0.19 (0.12; 0.33)	0.19 (0.12; 0.38)	0.18 (0.01; 0.19)	0.19 (0.11; 0.34)	0.18 (0.06; 0.29)	<0.001
Equipotent dosage lorazepam (mg/kg/day)	0.20 (0.10; 0.47)	0.20 (0.10; 0.20)	0.40 (0.20; 0.60)	0.60 (0.40; 1.00)	0.2 (0; 0.60)	0.40 (0.20; 0.47)	0.20 (0.04; 0.40)	<0.001
Sections with other sedatives used	147 (24)	17 (9)	42 (21)	28 (33)	22 (42)	14 (29)	22 (54)	<0.001

PIM II; Paediatric Index of Mortality score II, PRISM; Pediatric RIsk of Mortality score II, PICU; pediatric intensive care unit. Data are expressed as median (first quartile; third quartile) or number (percentage).

3.1 aEEG amplitude

For sections with CNV, we observed a significant ($p < 0.001$) increase in mean upper and lower band of the amplitudes with increasing age (Figure 9 and Appendix Figure 11 A-C). A majority of the patients (89%) displayed the same background pattern for all the studied nights. For 13 patients, the background pattern changed in the studied nights. Half of these patients started with DNV patterns that converted into CNV. An increasing number of ventilation days showed a decreasing trend on the average amplitude of the CNV sections.

The slope of the linear regression was significantly non-zero ($p < 0.05$) in the 0-1 month, 6-12 months, and 2-5 years groups (Appendix Figure 12). A decreasing trend was observed in average amplitude for an increasing equipotent Lorazepam dosage with a significantly non-zero ($p < 0.05$) regression slope for the 0-1 month and 5-18 years age group (Appendix Figure 13). The equipotent Methadone dosage did not affect the average amplitude of the CNV sections (Appendix Figure 14).

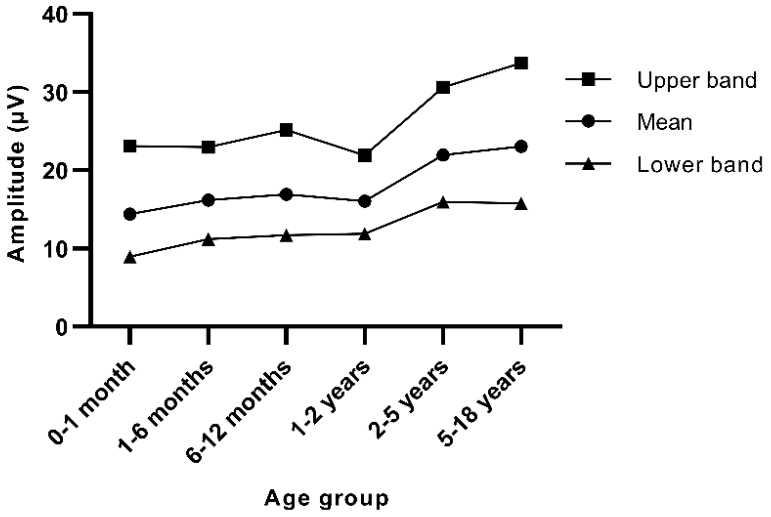

Figure 9: *Median data of the average section amplitude, average section upper band, and average section lower band for all the CNV sections.*

3.2 SWC analysis

Figure 10 graphically summarises the presence or absence of SWC stratified by age, total values can be found in Appendix Table 5. SWC were mainly observed in patients < 2 years of age ($p < 0.001$). The equipotent lorazepam influenced the presence of SWC in the 0-1 month age group ($p = 0.001$). The sections without SWC had the highest dosage of lorazepam, followed by the SWC sections, and the imminent/immature sections had the lowest dosage. No influence was seen in the other age groups or compared to the equipotent methadone dosage and days spent on the ventilator. When comparing the first half of the study period (first days, sections 1-5) with the later stages (last days, sections 6-10), the 0-1 month group had a higher portion of sections without SWC in the first five sections (25% vs 4%) and a lower portion of SWC (48% vs 69%) when comparing to the later five sections ($p = 0.038$).

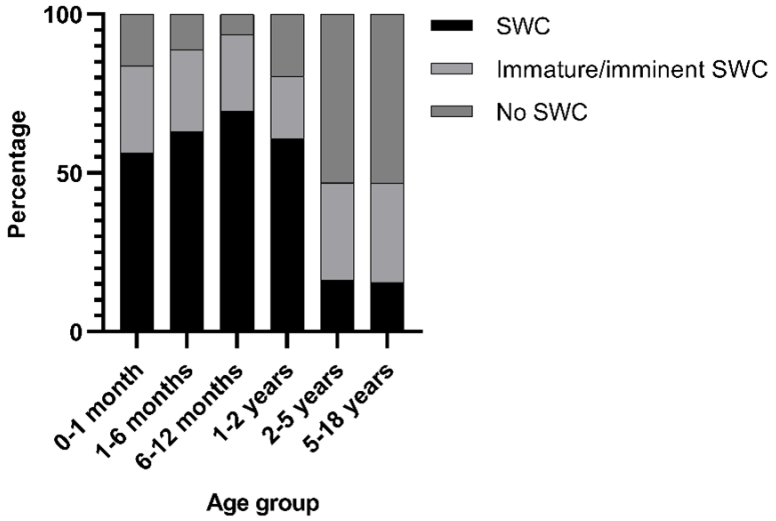

Figure 10: *Relative occurrence of the different SWC types in sections with CNV.*

3.3 Automatic classification of SWC

All the features used for the classification model (number of changes, complete cycles, standard deviation, and ApEN) were statistically different between the different groups (”SWC present”, ”Imminent/immature SWC”, and ”no SWC present”) with a p-value < 0.0001 (Appendix Figure 15). The model with three outcome parameters had an overall accuracy of 70.1% and an AUC of the ROC curve of 92%. The confusion matrix of this model is shown in Table 2. The model with two outcome variables, where the imminent/immature SWC and SWC are grouped, had an improved accuracy of 87.7% and an AUC of the ROC curve of 0.92. The confusion matrix is shown in Table 3, which results in a sensitivity of 90.8% and a specificity of 75.2%.

Table 2: *PIM II; Paediatric Index of Mortality score II, PRISM; Pediatric RIsk of Mortality score II, PICU; pediatric intensive care unit. Data are expressed as median (first quartile; third quartile) or number (percentage).*

Actual \ Predicted	No SWC present	Imminent/immature SWC	SWC present
No SWC present	75	23	11
Imminent/immature SWC	28	53	68
SWC present	4	32	261

Table 3: *PIM II; Paediatric Index of Mortality score II, PRISM; Pediatric RIsk of Mortality score II, PICU; pediatric intensive care unit. Data are expressed as median (first quartile; third quartile) or number (percentage).*

Predicted / Actual	No SWC present	Some form of SWC present
No SWC present	82	27
Some form of SWC present	41	405

Chapter 4

Discussion

To our knowledge, this is the first study describing aEEG background patterns and the presence of SWC in mechanically ventilated children aged 0-18 years. We demonstrated that the amplitude of aEEG increases significantly with age and that SWC are most commonly seen until two years. The results shown in this study can be of clinical value for the paediatric critical care that utilise aEEG. It will be easier to interpret the aEEG recordings in this population and help differentiate the physiological background patterns from pathological patterns, such as DNV or BS [25]. Furthermore, the results allow the study of the sleep pattern in mechanically ventilated children in the PICU. On top of that, the results of the classification model with two outcome parameters indicate that the presence of SWC can be automatically classified and used in further applications, such as studying the sleep pattern.

4.1 aEEG amplitude

The results for the 0-1 month group are comparable to previous studies. The observed CNV amplitudes of the upper and lower band are in line with the classification of CNV used in (pre)mature infants, with a lower amplitude below 10μV and an upper amplitude between 10-25μV [18], [29]. The results of the older age groups are more difficult to compare to previous studies due to the lack of research in the paediatric population. One study created reference values for infants up to 3.5 months, which are comparable to the 1-6 months group [22]. The study found an increase in amplitude with increasing age. The absolute values of the amplitudes of the upper and lower band are similar but differ slightly. A depressing effect of sedatives like midazolam and morphine on aEEG amplitude has been described before [29], [30]. This depressing effect was also seen with the equipotent lorazepam dosage in the 0-1 month age group, but not in the other age groups. However, a depressing effect of morphine or fentanyl was not seen in the equipotent methadone dosage, while it is described in (pre)mature infants [29], [30].

4.2 SWC analysis

It can be seen that with the background classification of Hellström-Westas [18] most of the background patterns in each age group are CNV. DNV is only seen in a significant amount in the 0-1 month group. The trend in Figure 3 can explain this lack of DNV in the other age groups. For the groups between 1 month and two years, the median amplitudes increase with an average of 2.5μV. For the age groups between 2-18 years, the median amplitudes increase with an average of 5-6μV. This increase in amplitude can have a significant impact on background pattern classification. For example, for the classification of DNV, the lower band has to have an amplitude below 5μV. If the patient's age can increase the amplitude by 2.5-5μV, it is logical that the DNV pattern is rarely seen in the older age groups. It is, however, also possible that the more developed brain of the older age groups does not generate DNV patterns.
Frequent trends were seen in the 0-1 month age group that were not seen in the older age groups. For instance, the relation of equipotent lorazepam dosage with decreasing amplitude and presence of SWC. These relations were not found in the older age groups, this further signifies the necessity for more research on aEEG in the older age groups, as the knowledge of the neonatal care, as well as the adult care, cannot completely be translated to the paediatric population.
The occurrence of SWC in the age groups up to 2 years is similar, around 50%. After this, the occurrence of SWC drops to about 15%. The decrease in SWC is compensated by the significant increase of no SWC and a slight increase of imminent/immature SWC. The logic behind this decrease at this age is unknown. However, it is most likely that at this age, the sleep-wake cycling develops into a more adult sleep-wake pattern without the distinct SWC, as the sleep architecture of children changes in the first years [19].

4.3 Automatic classification of SWC

The accuracy in the detection of SWC of the two different classification models was different, 70.1% vs 87.7%. This change in accuracy is mainly contributed to the relatively bad detection of the 'Imminent/immature SWC' group in the classification model with three outcome variables, the positive predictive value for this group is below 50%. This could be addressed by making the model more complex or adding a feature with more discriminating power in this group. However, the model in which the SWC groups are combined into 'some form of SWC present' performs much better. The sensitivity and specificity found in this study (90.8% and 75.2%, respectively) are similar, if not better, than the sensitivity and specificity found in a previous study (81.3 and 75.3, respectively) which used a similar classification of SWC groups with two variables.

4.4 Study limitations

Some limitations of this study need to be discussed. First, the official algorithms used in aEEG monitors are proprietary and mostly unknown [16], [17], [31]. In this study, the WU-NEAT algorithm is used for generating aEEG waveforms from the available EEG measurements [17]. The use of the algorithm may influence the results generated in this study. For instance, the final processing step in the algorithm is to offset the aEEG by one to mimic the higher voltage aspects more accurately in the signal. This offset by 1 could significantly affect the amplitude of the lower band or the labelling of DNV sections, where the lower band should be above 5μV.
Secondly, the data selection could bias the results found in this study. All the data is recorded during the night to minimise the effect of artefacts in the signals. This selective data usage could skew the SWC data in groups with a more developed circadian rhythm and sleep more during the nights. This would include all the groups except the 0-1 month group, as the circadian rhythm is thought to develop between 2-4 months [32], [33].
Thirdly, because the study is a secondary analysis of prospectively collected data, the parameters that could influence the measurements are unknown. For instance, it is unknown whether the cyclic variation seen in the imminent/immature groups is caused by changes in sleep-wake pattern or other factors like motion artefacts. This could explain why the imminent/immature group had the lowest equipotent Lorazepam dosage, as a lower Lorazepam dosage could indicate lower sedation and therefore more movement artefacts. Finally, the number of patients in the different age groups differs substantially. The largest group, 1-6 months, consists of 37 patients and 196 sections, while the smallest group, 5-18 years, only has nine patients and 45 sections. This may cause the values reported for these age groups to be the least representative. This is, however, inherent to the population of the studied PICU, as the patient population follows the same age distribution.

Chapter 5

Conclusion

In conclusion, this study demonstrates that the amplitude of the aEEG increased with age, that prolonged ventilation correlates with lower aEEG amplitudes, and that SWC were commonly seen till the age of 2 years. The automated detection of SWC shows potential to be utilised in further projects and will allow for a more accessible quantitative measure of sleep; however, further optimising might be needed. With these results, an adjusted background pattern classification could be created to counteract this increase in amplitude. Such an adjusted classification could be of clinical significance in the paediatric population, but further research is required to test an adjusted classification.

Bibliography

[1] G. Rees, J. Gledhill, M. E. Garralda, and S. Nadel, "Psychiatric outcome following paediatric intensive care unit (PICU) admission: A cohort study," *Intensive Care Medicine*, vol. 30, no. 8, pp. 1607–1614, 2004. [Online]. Available: https://pubmed.ncbi.nlm.nih.gov/15112035/

[2] S. R. Kudchadkar, O. A. Aljohani, and N. M. Punjabi, "Sleep of critically ill children in the pediatric intensive care unit: A systematic review," pp. 103–110, 4 2014. [Online]. Available: /pmc/articles/PMC3883975//pmc/articles/PMC3883975/?report=abstracthttps://www.ncbi.nlm.nih.gov/pmc/articles/PMC3883975/

[3] A. Calandriello, J. Tylka, and P. Patwari, "Sleep and Delirium in Pediatric Critical Illness: What Is the Relationship?" *Medical Sciences*, vol. 6, no. 4, p. 90, 10 2018. [Online]. Available: /pmc/articles/PMC6313745//pmc/articles/PMC6313745/?report=abstracthttps://www.ncbi.nlm.nih.gov/pmc/articles/PMC6313745/

[4] W. Medrzycka-Dabrowska, K. Lewandowska, K. Kwiecień-Jagus, and K. Czyz-Szypenbajl, "Sleep deprivation in Intensive Care Unit-systematic review," *Open Medicine (Poland)*, vol. 13, no. 1, pp. 384–393, 1 2018. [Online]. Available: /pmc/articles/PMC6132084//pmc/articles/PMC6132084/?report=abstracthttps://www.ncbi.nlm.nih.gov/pmc/articles/PMC6132084/

[5] F. G. Beltrami, X. L. Nguyen, C. Pichereau, E. Maury, B. Fleury, and S. Fagondes, "Sleep in the intensive care unit," *Jornal Brasileiro de Pneumologia*, vol. 41, no. 6, pp. 539–546, 12 2015.

[6] I. Telias and M. E. Wilcox, "Sleep and Circadian Rhythm in Critical Illness," pp. 1–8, 3 2019. [Online]. Available: https://doi.org/10.1186/s13054-019-2366-0

[7] J. A. Berger and S. R. Kudchadkar, "Sleep in the Pediatric Intensive Care Unit," *Sedation and Analgesia for the Pediatric Intensivist*, pp. 259–273, 2021. [Online]. Available: https://link-springer-com.proxy-ub.rug.nl/chapter/10.1007/978-3-030-52555-2_19

[8] N. C. Corser, "Sleep of 1- And 2-Year-old Children in Intensive Care," *Comprehensive Child and Adolescent Nursing*, vol. 19, no. 1, pp. 17–31, 1996. [Online]. Available: https://pubmed.ncbi.nlm.nih.gov/8920497/

[9] R. E. Sanchez, J. E. Wrede, R. S. Watson, H. O. de la Iglesia, and L. A. Dervan, "Actigraphy in mechanically ventilated pediatric ICU patients: comparison to PSG and evaluation of behavioral circadian rhythmicity," *https://doi.org/10.1080/07420528.2021.1987451*, 2021. [Online]. Available: https://www.tandfonline.com/doi/abs/10.1080/07420528.2021.1987451

[10] C. Chen, C. Sun, S. Leonhardt, P. Andriessen, H. Niemarkt, and W. Chen, "Amplitude-Integrated Electroencephalography Applications and Algorithms in Neonates: A Systematic Review," pp. 141 766–141 781, 2019.

[11] D. Azzopardi, "Clinical applications of cerebral function monitoring in neonates," *Seminars in Fetal and Neonatal Medicine*, vol. 20, no. 3, pp. 154–163, 2015. [Online]. Available: http://dx.doi.org/10.1016/j.siny.2015.02.001

[12] H. Kidokoro, T. Inder, A. Okumura, and K. Watanabe, "What does cyclicity on amplitude-integrated EEG mean," *Journal of Perinatology*, vol. 32, no. 8, pp. 565–569, 8 2012.

[13] J. D. Tao and A. M. Mathur, "Using amplitude-integrated EEG in neonatal intensive care," *Journal of Perinatology*, vol. 30, no. SUPPL. 1, pp. 73–81, 2010.

[14] N. A. Shah and C. J. Wusthoff, "How to use: Amplitude-integrated EEG (aEEG)," *Archives of Disease in Childhood: Education and Practice Edition*, vol. 100, no. 2, pp. 75–81, 2015.

[15] D. Maynard, P. F. Prior, and D. F. Scott, "Device for Continuous Monitoring of Cerebral Activity in Resuscitated Patients," *British Medical Journal*, vol. 4, no. 5682, pp. 545–546, 11 1969. [Online]. Available: https://www.ncbi.nlm.nih.gov/pmc/articles/PMC1630343/

[16] D. Zhang and H. Ding, "Calculation of compact amplitude-integrated EEG tracing and upper and lower margins using raw EEG data," *Health*, vol. 05, no. 05, pp. 885–891, 5 2013. [Online]. Available: http://dx.

[17] Z. A. Vesoulis, P. G. Gamble, S. Jain, N. M. E. Ters, S. M. Liao, and A. M. Mathur, "WU-NEAT: A clinically validated, open- source MATLAB toolbox for limited-channel neonatal EEG analysis," 5 2018. [Online]. Available: http://arxiv.org/abs/1805.04566

[18] L. Hellstro m-Westas, I. Rosen, L. S. de Vries, and G. Greisen, "Amplitude-integrated EEG Classification and Interpretation in Preterm and Term Infants," *NeoReviews*, vol. 7, no. 2, pp. e76–e87, 2 2006. [Online]. Available: https://neoreviews.aappublications.org/content/7/2/e76https://neoreviews.aappublications.org/content/7/2/e76.abstract

[19] J. E. MacLean, D. A. Fitzgerald, and K. A. Waters, "Developmental changes in sleep and breathing across infancy and childhood," pp. 276–284, 9 2015.

[20] L. Curzi-Dascalova, P. Peirano, and F. Morel-Kahn, "Development of sleep states in normal premature and full-term newborns," *Developmental Psychobiology*, vol. 21, no. 5, pp. 431–444, 1988. [Online]. Available: https://pubmed.ncbi.nlm.nih.gov/3402666/

[21] S. Chokroverty, “Overview of sleep & sleep disorders,” Tech. Rep., 2010. [Online]. Available: http://www.ijmr.org.in

[22] D. Zhang, Y. Liu, X. Hou, C. Zhou, Y. Luo, D. Ye, and H. Ding, “Reference values for amplitude-integrated EEGs in infants from preterm to 3.5 months of age,” *Pediatrics*, vol. 127, no. 5, 2011. [Online]. Available: https://pubmed.ncbi.nlm.nih.gov/21482614/

[23] D. Shah and A. Mathur, “Amplitude-Integrated EEG and the Newborn Infant,” *Current Pediatric Reviews*, vol. 10, no. 1, pp. 11–15, 2014.

[24] N. Bruns, U. Felderhoff-Müser, C. Dohna-Schwake, J. Woelfle, and H. Müller, “aEEG Use in Pediatric Critical Care—An Online Survey,” *Frontiers in Pediatrics*, vol. 8, no. 3, 1 2020. [Online]. Available: /pmc/articles/PMC6992599//pmc/articles/PMC6992599/?report=abstracthttps://www.ncbi.nlm.nih.gov/pmc/articles/PMC6992599/

[25] N. Bruns, U. Felderhoff-Müser, and C. Dohna-Schwake, “aEEG as a useful tool for neuromonitoring in critically ill children – Current evidence and knowledge gaps,” *Acta Paediatrica*, p. apa.15676, 12 2020. [Online]. Available: https://onlinelibrary.wiley.com/doi/10.1111/apa.15676

[26] R. Siddappa, J. E. Fletcher, A. M. Heard, D. Kielma, M. Cimino, and C. M. Heard, “Methadone dosage for prevention of opioid withdrawal in children,” *Paediatric Anaesthesia*, vol. 13, no. 9, pp. 805–810, 2003. [Online]. Available: https://pubmed.ncbi.nlm.nih.gov/14617122/

[27] J. D. Tobias, “Tolerance, withdrawal, and physical dependency after long-term sedation and analgesia of children in the pediatric intensive care unit,” pp. 2122–2132, 2000. [Online]. Available: https://pubmed.ncbi.nlm.nih.gov/10890677/

[28] M. L. McHugh, “Interrater reliability: The kappa statistic,” *Biochemia Medica*, vol. 22, no. 3, pp. 276–282, 2012. [Online]. Available: /pmc/articles/PMC3900052//pmc/articles/PMC3900052/?report=abstracthttps://www.ncbi.nlm.nih.gov/pmc/articles/PMC3900052/

[29] L. Hellström-Westas and I. Rosén, “Continuous brain-function monitoring: State of the art in clinical practice,” *Seminars in Fetal and Neonatal Medicine*, vol. 11, no. 6, pp. 503–511, 12 2006. [Online]. Available: http://www.sfnmjournal.com/article/S1744165X06000783/fulltexthttp://www.sfnmjournal.com/article/S1744165X06000783/abstracthttps://www.sfnmjournal.com/article/S1744-165X(06)00078-3/abstract

[30] V. Bernet, B. Latal, G. Natalucci, C. Doell, A. Ziegler, and G. Wohlrab, “Effect of sedation and analgesia on postoperative amplitude-integrated eeg in newborn cardiac patients,” *Pediatric Research*, vol. 67, no. 6, pp. 650–655, 6 2010. [Online]. Available: https://www.nature.com/articles/pr2010116

[31] T. Werther, M. Olischar, G. Naulaers, P. Deindl, K. Klebermass-Schrehof, and N. Stevenson, “Are All Amplitude-Integrated Electroencephalogram Systems Equal?” *Neonatology*, vol. 112, no. 4, pp. 394–401, 11 2017. [Online]. Available: https://pubmed.ncbi.nlm.nih.gov/28926828/

[32] J. Yates, “Perspective: The long-term effects of light exposure on establishment of newborn circadian rhythm,” pp. 1829–1830, 10 2018. [Online]. Available: /pmc/articles/PMC6175794//pmc/articles/PMC6175794/?report=abstracthttps://www.ncbi.nlm.nih.gov/pmc/articles/PMC6175794/

[33] K. McGraw, R. Hoffmann, C. Harker, and J. H. Herman, “The development of circadian rhythms in a human infant,” *Sleep*, vol. 22, no. 3, pp. 303–310, 5 1999. [Online]. Available: https://pubmed.ncbi.nlm.nih.gov/10341380/

Appendix

Table 4: *Number of background patterns per age group.*

	Sections CNV	Sections DNV	Sections BS
0-1 month	135	49	2
1-6 months	189	5	2
6-12 months	79	4	2
1-2 years	51	0	1
2-5 years	49	0	0
5-18 years	37	3	5

CNV; continuous normal voltage, DNV; discontinuous normal voltage, BS; burst suppression.

Table 5: *Absolute occurrence of SWC types for each age group.*

Age group	SWC	Immature/ imminent SWC	No SWC
0-1 month	76	37	22
1-6 months	119	49	21
6-12 months	55	19	5
1-2 years	31	10	10
2-5 years	8	15	26
5-18 years	5	10	17

SWC; sleep-wake cycle.

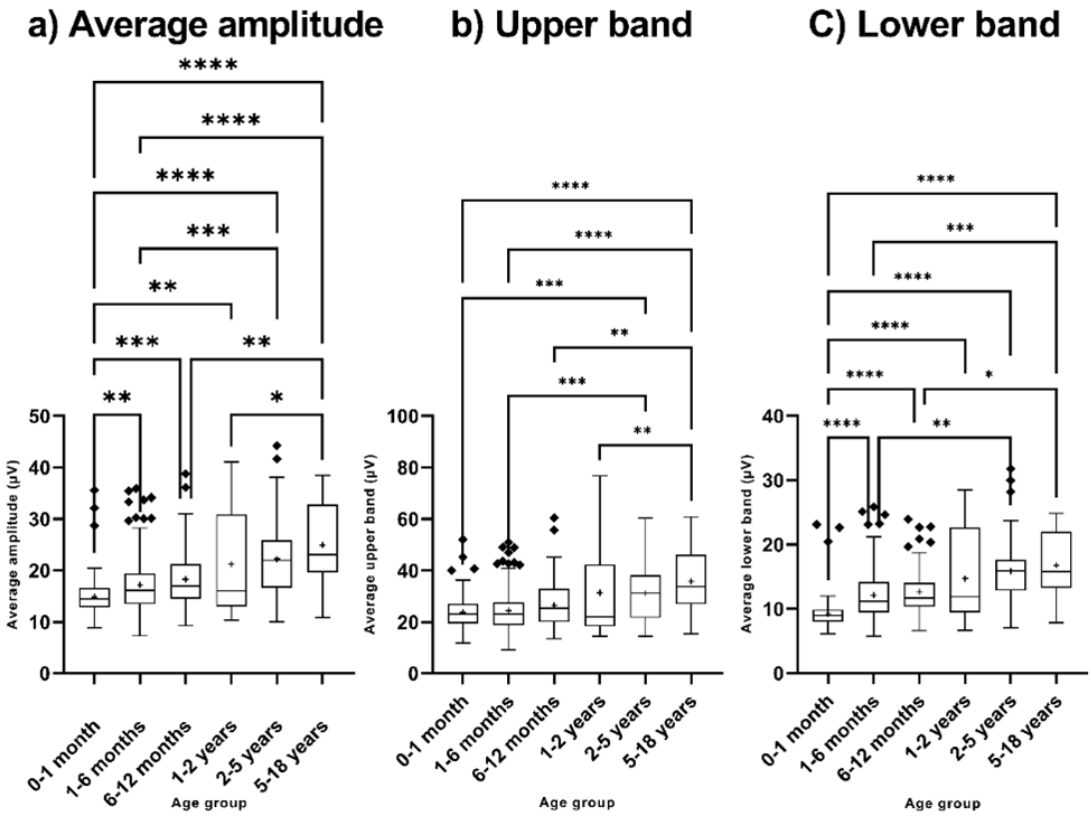

Figure 11: *Box plot of average (a), upper (b) and lower (c) band amplitude per age group. The median and interquartile range (IQR) are depicted in the boxplots, the mean is depicted as the plus symbol. Outliers are calculated with Tukey's fence method and are depicted outside the boxplots, the mean is depicted as the plus symbol. Outliers are calculated with Tukey's fence method and are depicted as diamonds. The asterisk indicate a statistical significant difference between the two groups (* p-value = 0.01 to 0.05, ** p-value = 0.001 to 0.01, *** p-value = 0.0001 to 0.001, **** p-value $<$ 0.0001).*

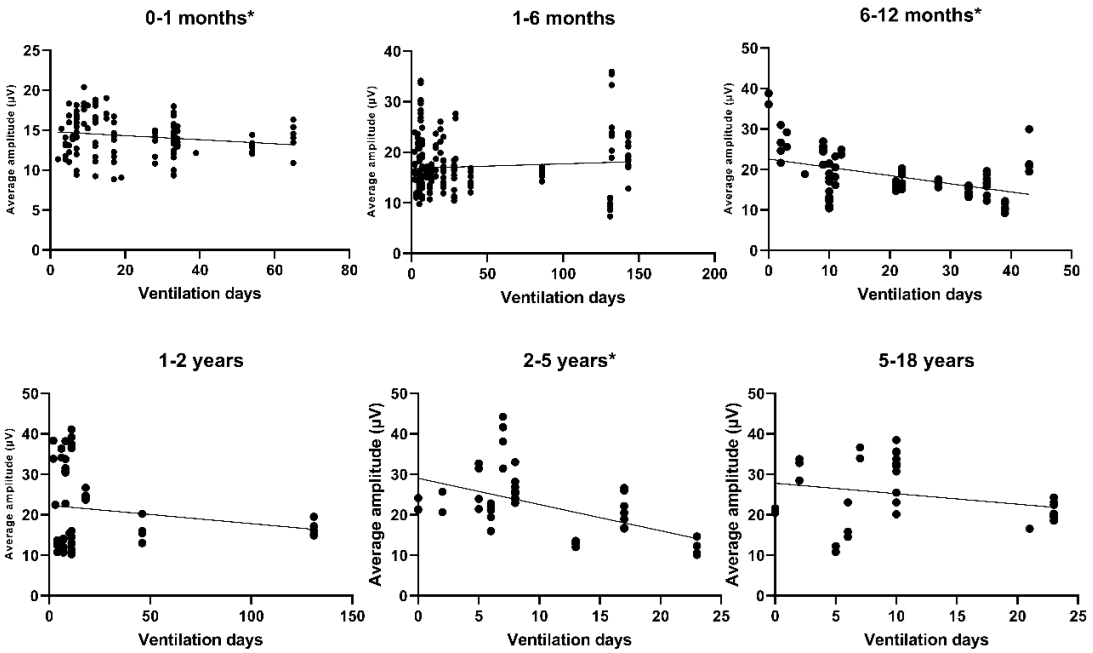

Figure 12: *The average amplitude of the CNV sections plotted against the ventilation days. A trend line is added, an asterisk in the title indicates a non-zero slope of the trend-line ($p < 0.05$).*

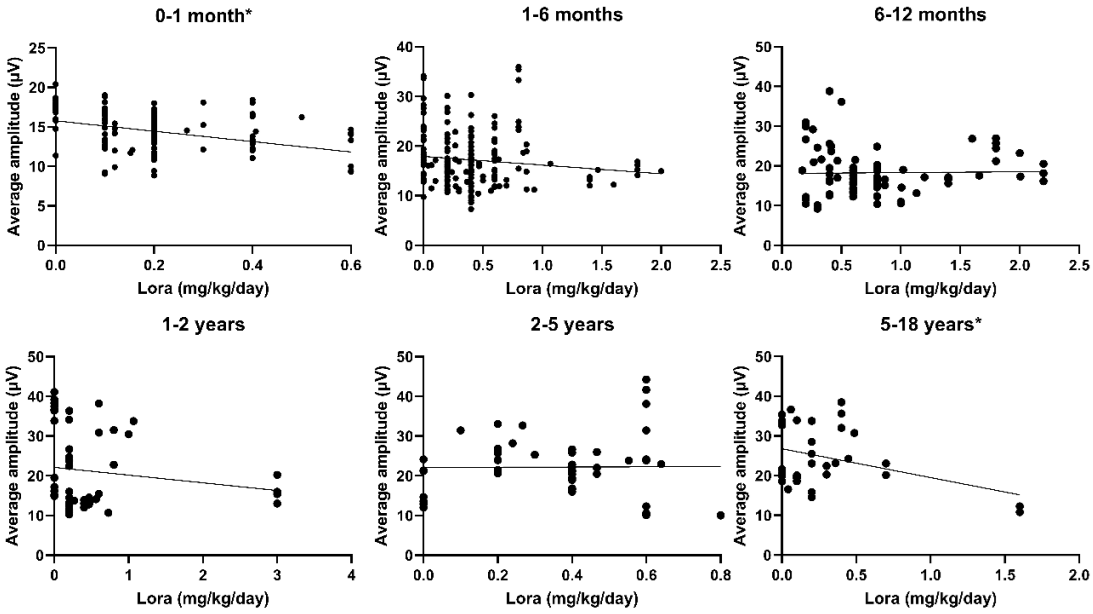

Figure 13: *The average amplitude of the CNV sections plotted against the equipotent lorazepam dosage. A trend line is added, an asterisk in the title indicates a non-zero slope of the trend-line ($p < 0.05$).*

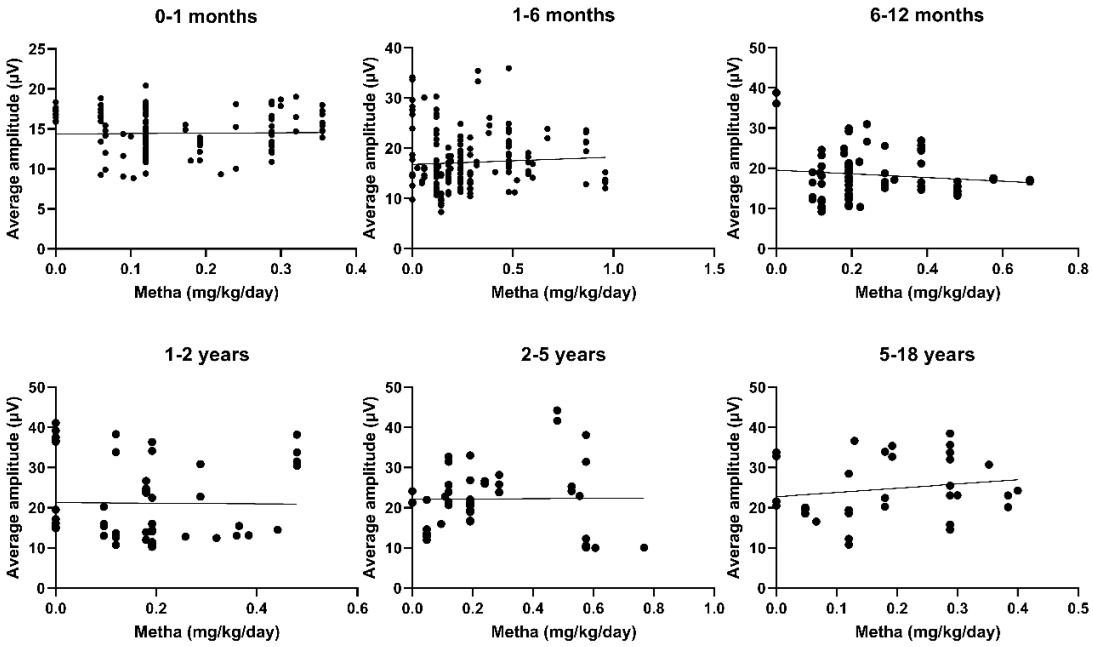

Figure 14: *The average amplitude of the CNV sections plotted against the equipotent methadone dosage. A trend line is added, an asterisk in the title indicates a non-zero slope of the trend-line ($p < 0.05$).*

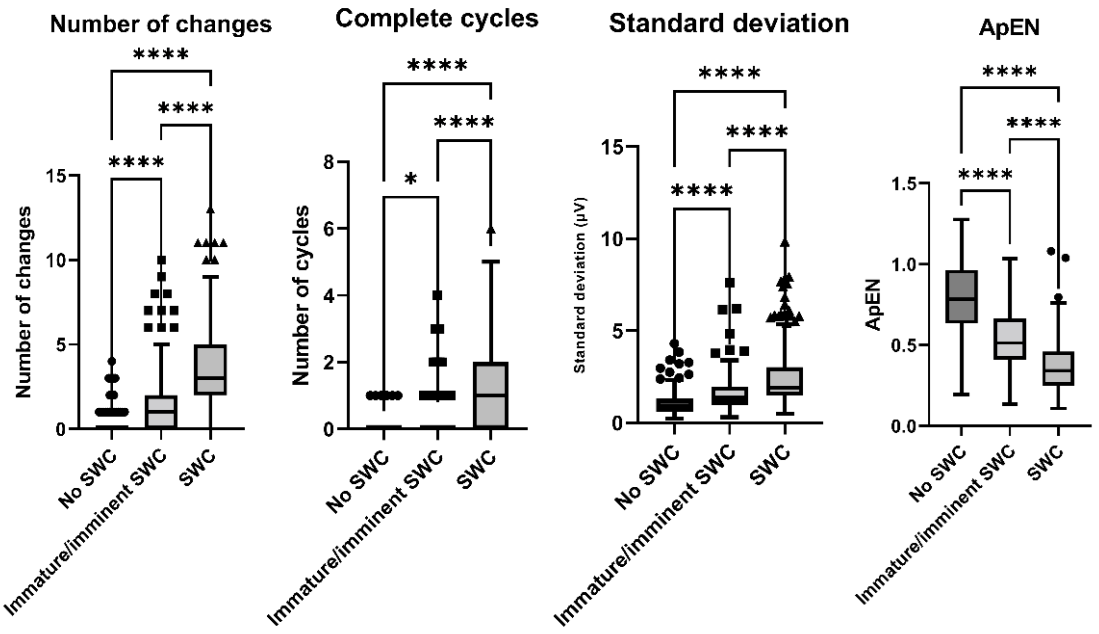

Figure 15: *Box plot of the features used in SWC classification model per SWC group. The median and interquartile range (IQR) are depicted in the boxplots. Outliers are calculated with Tukey's fence method and are depicted outside the boxplots, the mean is depicted as the plus symbol. Outliers are calculated with Tukey's fence method and are depicted as diamonds. The asterisk indicate a statistical significant difference between the two groups (* p-value = 0.01 to 0.05, ** p-value = 0.001 to 0.01, *** p-value = 0.0001 to 0.001, **** p-value $<$ 0.0001).*